

## ARTICLES

**Survey of elemental specificity in positron annihilation peak shapes**

U. Myler\* and P. J. Simpson

*Department of Physics and Astronomy, The University of Western Ontario, London, Ontario, Canada N6A 3K7*

(Received 14 April 1997)

Recently the detailed interpretation of positron-annihilation  $\gamma$ -ray peak shapes has proven to be of interest with respect to their chemical specificity. In this contribution, we show highly resolved spectra for a number of different elements. To this purpose, annihilation spectra with strongly reduced background intensities were recorded in the two detector geometry, using a variable-energy positron beam. Division of the subsequently normalized spectra by a standard spectrum (in our case the spectrum of pure silicon) yields quotient spectra, which display features characteristic of the sample material. First we ascertain that the specific spectrum of an element is conserved in different chemical compounds, demonstrated here by identical oxygen spectra obtained from both  $\text{SiO}_2/\text{Si}$  and  $\text{MgO}/\text{Mg}$ . Second, we show highly resolved spectra for a number of different elements (Fe . . . Zn, Ag, Ir . . . Au). We show that the characteristic features in these spectra vary in a systematic fashion with the atomic number of the element and can be tentatively identified with particular orbitals. Finally, for 26 different elements we compare the maximum intensity in the quotient spectra with the relative atomic density in the corresponding element. To our knowledge, this is the most comprehensive survey of such data made to date. [S0163-1829(97)03346-8]

**I. INTRODUCTION**

Positron-annihilation spectroscopy has matured into a powerful and versatile tool in materials analysis.<sup>1-3</sup> Generally, positrons are implanted into a material sample, where they thermalize very rapidly before they annihilate with an electron provided by a sample atom. The majority of annihilation events generate two  $\gamma$  quanta with energies of about 511 keV, emitted into close to opposite directions. The electron involved in the annihilation can either be a relatively free valence electron, or, depending on the sample material, a more or less strongly bound core electron. Since not only the total energy, but also the total momentum of the positron-electron pair must be conserved in the annihilation process, the resulting  $\gamma$  peak exhibits Doppler broadening. However, the momentum contribution of the thermalized positrons is negligible compared to the momenta of the electrons. Therefore the width and shape of the annihilation peak are independent of the positron source and the positron implantation process, and are dependent only on the electronic environment in which the positrons annihilate, i.e., the physical and chemical structure of the sample material.

Consequently, one way to probe materials with positrons is based on the measurement of the width of the annihilation  $\gamma$ -ray peak. This approach is frequently applied in connection with a positron beam facility, which makes it possible to irradiate the samples with a collimated beam of monoenergetic positrons. Since the implantation depth is determined by the positron energy, depth resolved measurements are possible. In the most common experimental setups, only one of the two annihilation quanta is measured with a Ge detector, resulting typically in a spectrum as

shown in Fig. 1(a). In the subsequent data analysis, the spectrum is parametrized by a single number, most frequently the "sharpness" parameter  $S$ , which is defined as the ratio of the counts in a central region of the peak (e.g., from 510.3 to 511.7 keV) to the total number of counts in the peak.<sup>1</sup> Since the central peak region is predominantly composed of annihilation events with low-momentum electrons (i.e., valence electrons, in contrast to core electrons, which are characterized by high momenta) changes of the  $S$  parameter reflect changes in the relative contributions of valence vs core electrons. For example, in the case that a positron is trapped by a vacancy, the relative contribution of valence electron annihilations will be increased as compared to the defect-free material, giving rise to an increase of  $S$ .

The determination of  $S$  as a function of positron energy and especially the analysis of the changes of these  $S(E_{\text{positron}})$  curves in response to a variety of sample treatments (e.g., thermal and mechanical) continues to supply new and interesting insights into material structures. However, the information contained in the annihilation  $\gamma$ -ray spectra is by no means fully utilized when only the  $S$  parameter is extracted. Rather, a detailed analysis of the annihilation peak shows that the intensity as a function of  $\gamma$  energy is slightly different for materials of different chemical composition, since the spectrum is a "sampling" of the electron momentum distribution. In the region of the peak made accessible by the two detector technique, annihilations with core electrons account for the majority of events, and therefore the characteristic core electron structure with its differences in orbital occupation as well as electron binding and kinetic energies gives rise to a slightly different peak shape for every single element. Detailed analysis of annihilation

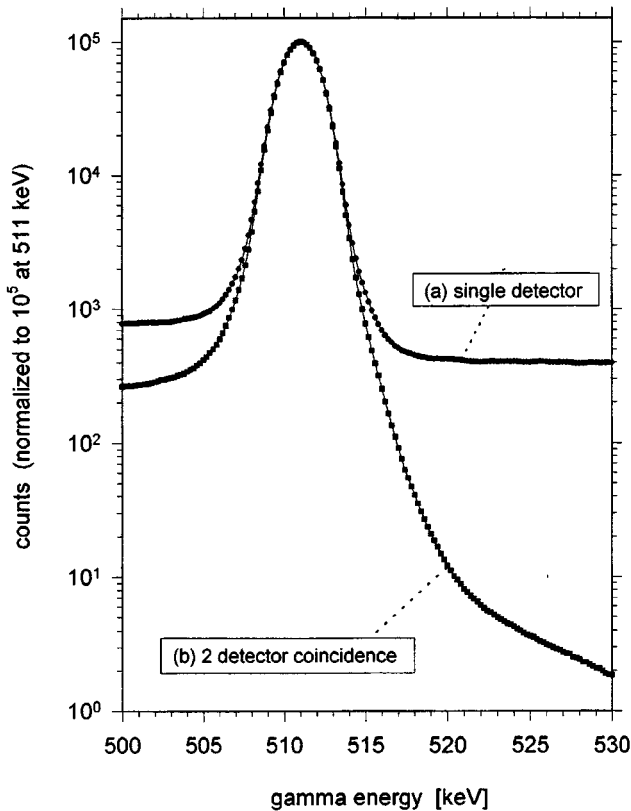


FIG. 1. Positron-electron annihilation peak in silicon (a) as recorded with a Ge detector only, and (b) measured with the same detector, but in coincidence with signals from NaI scintillation detector on the opposite side of the sample. Positron energy: 40 keV.

peak shapes has only recently regained attention<sup>4-8</sup> after its initial introduction about 20 years ago.<sup>9-12</sup>

A major problem when trying to analyze the flanks of single detector annihilation spectra is the poor peak to background ratio of roughly 250 [compare Fig. 1(a)]. The background on the high-energy side of the peak has several causes. In the case of using <sup>22</sup>Na as a positron source, a  $\gamma$  quantum with an energy of 1.275 MeV is emitted together with the positron. Some of these quanta, after several scattering processes, may enter the detector, giving rise to a background that is practically flat in the 511 keV region we are interested in. Also, at higher count rates, pulse pileup contributes to the background. Another common source of high- and low-energy background, of course, is cosmic radiation. On the low-energy flank of the peak, scattering of the annihilation quanta and incomplete charge collection in the detector causes an intense additional background component. In order to get accurate information about high-energy core electrons, the energy range in which the annihilation peak can be analyzed has to be extended.

This is possible by using the two detector geometry as described by Lynn and Goland.<sup>9</sup> Here, another detector is added collinearly with the first at the opposite side of the sample. Only those events of the first detector that are accompanied by a coincidence count in the second detector are accepted. Since in this setup the signal from the second detector is not used for a precise energy determination, but only to decide if a second  $\gamma$  quantum was emitted at the same

time into roughly the opposite direction (and therefore the event is most likely a real annihilation event), the energy resolution of the second detector does not influence the energy resolution of the spectrum. Therefore a NaI(Tl) scintillation detector may be used. Figure 1(b) shows a spectrum obtained with this configuration. Clearly, on the high-energy side the background is reduced by a factor of about 200 at 530 keV. The reduction on the low-energy side is not as dramatic, because the effects of scattering, incomplete charge collection, and 3- $\gamma$  positronium decay cannot be remedied by the second detector. Therefore, in the following we are analyzing only the high-energy flank. With this setup, we obtain a peak to background ratio of almost  $10^5$ .

## II. EXPERIMENTAL

Measurements were carried out using the variable-energy positron beam facility at the University of Western Ontario.<sup>13</sup> Briefly, positrons emitted from a <sup>22</sup>Na source of (currently) 68 mCi are moderated to energies of about 3 eV and electrostatically accelerated to a preselected energy between 500 eV and 60 keV, while guided onto the sample by an axial magnetic field. With the vacuum system usually not being baked, the measurements are performed at a pressure of about  $10^{-7}$  Torr.

The main detector is a 210 cm<sup>3</sup> HP Ge detector with a resolution of about 1.3 keV at 511 keV. The auxiliary detector supplying the coincidence signals is a cylindrical 5"×5" NaI(Tl) scintillator crystal attached to a photo multiplier. The two detectors face each other at right angles to the direction of the incident positron beam. During the measurement, the sample surface normal is tilted about 10° towards the Ge detector, so that the annihilation  $\gamma$  quanta that are to be analyzed in the Ge detector do not suffer unnecessary absorption in the sample material. The data show that even in the coincidence mode the background count rate can be significantly reduced by thoroughly shielding both detectors with lead, resulting in a peak to background ratio of almost  $10^5$ , somewhat higher than other published results obtained with a scintillation counter as the auxiliary detector,<sup>4,5</sup> although our count rate is rather low.

In the configuration described above, we get a coincidence count rate of about 120/sec. The coincidence spectra were usually taken until about  $10^7$  counts had accumulated in the peak, which required about 24 h.

After a spectrum had been recorded, the energy scale of the system was calibrated by taking the position of the 662 keV  $\gamma$  line supplied by a small <sup>137</sup>Cs source in the single detector mode. Using the positions of the 511 and 662 keV peaks, the multichannel analyzer channels were converted into keV. In these spectra, each channel was about (but not exactly) 0.1 keV wide. In order to get comparable spectra for further analysis, these raw spectra were used to interpolate values with exactly 0.1 keV steps. Usually, a simple smoothing routine (averaging over  $n$  channels, with  $n$  increasing from 9 to 21 between 511 and 530 keV) was applied and finally the spectra were normalized to  $10^5$  counts in the 511.0 keV channel.

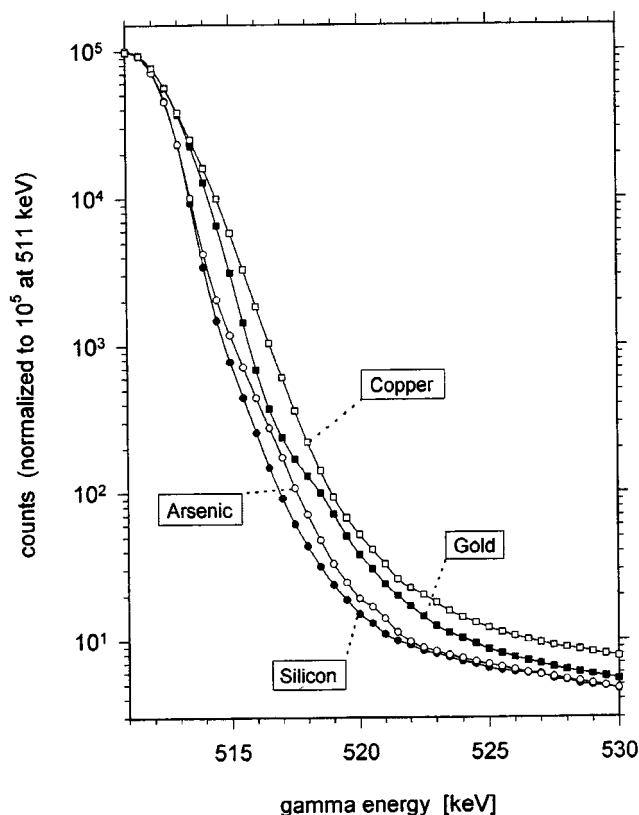


FIG. 2. High-energy half of annihilation peak after smoothing and normalization for samples of pure silicon, arsenic, gold and copper. Positron energy: 40 keV.

Figure 2 shows the results of this procedure for four elements with very different peak shapes: silicon, arsenic, gold, and copper. However, it is apparent that this method of depiction is not ideally suited for displaying the differences between the elements, or, even more so, to use them for quantitative evaluations. A way to overcome this drawback is the calculation of quotient spectra.<sup>5</sup> This is done by dividing the number of counts in each channel of the smoothed and normalized spectra by the number of counts in the corresponding channel of a "standard spectrum." Rather than using a synthetic function (e.g., a sum of gaussian and parabolic peaks), we found it advantageous to take the spectrum of a real sample as the standard. In this way, slight changes in the experimental setup (e.g., different distances or shielding geometries, which are possible since we use the two detector geometry only intermittently, and which mainly cause changes in the background level) can easily be accounted for experimentally by taking a new spectrum of the standard sample, thus getting "quotient spectra" that can be compared universally.

As a material which is readily available with high purity and single crystalline structure, we arbitrarily chose the spectrum of a virgin silicon (100) wafer (Czochralski type, phosphorus doped, resistivity 1–1.7  $\Omega$  cm) as the standard. Incidentally, we found that (at least for virgin Si), the dopant type and concentration has no perceptible effect on the peak shape. Care was taken to always orient the Si reference sample with the (001) axis toward the Ge detector. However, we expect the differences due to different crystallographic

orientations to be small in the energy range we are interested in. The choice of a different reference material would, of course, yield different quotient curves.

For the different elements under investigation single crystalline samples were used where available (Fe, Co, Ni, Zn, and Ir). Samples of Cu, Ag, Pt, and Au were polycrystalline sheets. Before taking the spectrum, the Cu sample was annealed at 900 °C for one hour; Ag, Pt, and Au foils were used as received. Vacancy-type defects in the samples may reduce the fraction of core annihilations and thereby reduce the peak heights in the quotient spectra (see below). The magnitude of this effect may be of the order of 10%. However, the peak shapes and therefore the trends discussed below should not be affected significantly.

### III. RESULTS

First we address the elemental specificity of quotient spectra, using oxygen as a test case. We have previously reported quotient spectra from a virgin Si standard sample for a range of positron energies and derived the oxygen contribution from the limiting case of very low positron energies ( $E_{\text{pos}} < 1$  keV), for which virtually all positrons annihilate within the native surface oxide layer.<sup>6</sup> We found a peak at 514.2 keV with a high-energy shoulder to be characteristic for the oxygen. In order to support the interpretation that this spectrum is actually the "fingerprint" of oxygen, we now report spectra of crystalline quartz ( $\text{SiO}_2$ ), magnesium, and crystalline magnesium oxide.

Figure 3 shows the resulting quotient spectra  $\text{SiO}_2/\text{Si}$  and  $\text{MgO}/\text{Mg}$ . Except for a difference in the maximum intensity, which is higher for the  $\text{MgO}/\text{Mg}$  curve by a factor of about 1.7, the general shape of the two quotient spectra is identical, and also reproduces the results attributed in Ref. 6 to the oxygen within the silicon surface oxide layer. We can therefore assume that these spectra, with a peak at 514.2 keV as the predominant feature, are indeed due to oxygen. This seems plausible, too, since the core electrons, which are mostly responsible for these spectra, are likely to be unaffected by different chemical environments of the oxygen atoms. The difference in intensities, on the other hand, can be tentatively attributed to a difference in the charge state of the oxygen:  $\text{MgO}$  is an ionic crystal, where the oxygen is present in the form of  $\text{O}^{2-}$  ions, while in the  $\text{SiO}_2$  the bonding is covalent, with only a partial negative charge on the oxygen due to the difference in electronegativity between oxygen and silicon. Therefore, in the  $\text{MgO}$  crystal, the positrons are more strongly attracted to the oxygen atoms than in the quartz and thus annihilate more frequently in the vicinity of oxygen, with the result that the oxygen-related signal is stronger in the spectrum of  $\text{MgO}$ , in contrast to what would be expected considering merely the stoichiometries.

We take this result as a further support for the previously reported conclusion, that elementally specific spectral features are conserved regardless of the elemental and structural environment (see, e.g., Ref. 6, where we show the similarity of spectra obtained from bulk samples and from silicon containing the same element as an impurity). We cannot actually prove, however, that this should be true for every material.

Assuming elemental specificity of the quotient spectra, it makes sense to conduct a systematic survey of characteristic

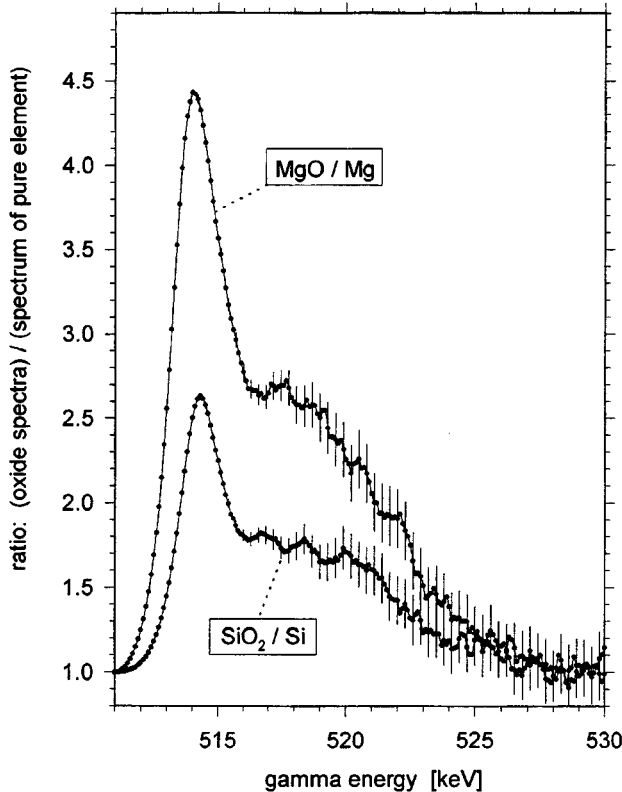


FIG. 3. Comparison of quotient spectra  $\text{SiO}_2/\text{Si}$  and  $\text{MgO}/\text{Mg}$ . All four original spectra are taken with a positron energy of 40 keV from bulk samples of the indicated material.

spectra throughout the periodic table. A few quotient spectra have already been published,<sup>5–8</sup> and differences between elements are readily visible. However, Szpala *et al.*<sup>5</sup> report that the quotient curves for Ni and Cu are identical at least within the energy range of their investigation (511–520 keV).

Therefore, among many other elements, we have measured well-resolved spectra for a number of transition metals: Fe, Co, Ni, Cu, and Zn as examples of 3d metals, Ag as a 4d metal, and Ir, Pt, and Au in the 5th period of the periodic table.

Concentrating first on the 3d metals Fe...Zn, Fig. 4 shows that there are in fact distinct systematic differences in the quotient spectra (contrary to Ref. 5). For clearer comparison, we have normalized the quotient curves to a value of 2 in the maximum; the maxima in the quotient curves as measured are 3.9 (Fe), 5.1 (Co), 7.8 (Ni), 7.75 (Cu), and 4.9 (Zn); compare Fig. 7.

As a simple method to parametrize these results, we further subtract the constant reference value of 1, and fit all spectra with 3 gaussians, see Figs. 5(a)–5(e). For all spectra the sum of the three gaussians is practically indistinguishable from the measured data except for energies above 520 keV, where due to the lowest count rates the measured curves exhibit the biggest statistical scatter. In Fig. 6 we show (a) the energies, and (b) the relative intensities of the 3 gaussian components  $G_1 \dots G_3$  ( $G_1$  being the narrow low energy,  $G_2$  the medium energy, and  $G_3$  the broad high-energy compo-

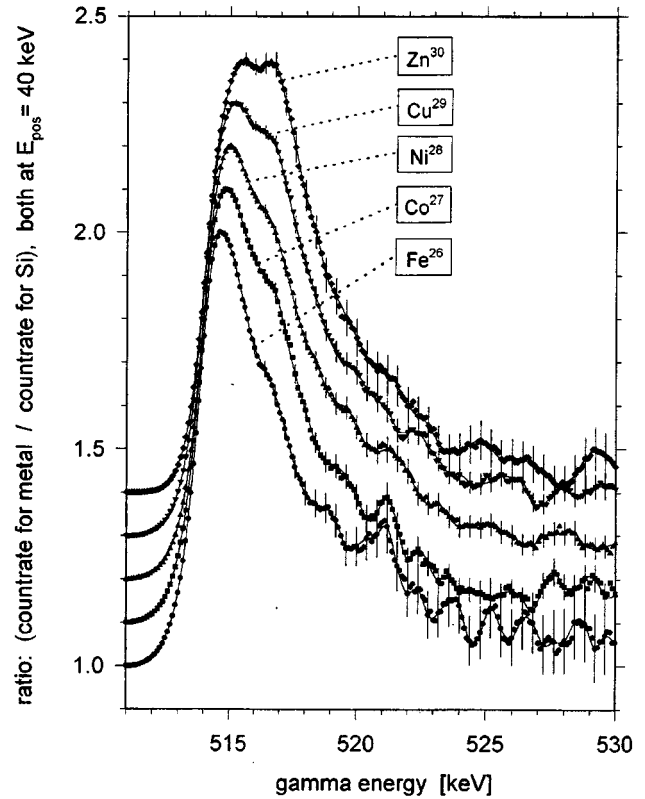


FIG. 4. Quotient spectra for the 3d metals Fe, Co, Ni, Cu, and Zn, divided by the standard Si spectrum, normalized to a maximum value of 2, and for clarity shifted by 0.1 each. Again, all spectra are taken with  $E_{\text{pos}} = 40$  keV.

nents in the fits). Clearly, all displayed values change monotonically with increasing atomic number  $Z$ . The increased variations in the center position of the  $G_3$  gaussians are explicable by the fact that this gaussian is much broader than the others and also represents the parts of the spectra with the lowest count rate and therefore the biggest relative errors.

Figure 5 also shows the normalized quotient curves for the other metals mentioned. While Ag exhibits the same general shape as the 3d metals, the spectra for Ir, Pt, and Au look quite different, but similar to each other.

Finally, in Fig. 7 we display the maximum intensities in the quotient spectra as a function of atomic number  $Z$ . We also show the relative number of atoms per  $\text{cm}^3$ . This curve was obtained by calculating the number of atoms per  $\text{cm}^3$  from the atomic weight and density of each element, and dividing these by the value for silicon. Surprisingly, it obviously describes the effective electron density responsible for shallow core-level annihilation processes, which are the main source of counts in the energy range of our quotient curves.

#### IV. DISCUSSION

In this contribution, we take an entirely phenomenological approach to positron-annihilation line shape analysis by simply showing experimental results. We hope to fulfil two goals: (i) to provide spectra for a broad range of elements, to be used as a test of theory, and (ii) to obtain a measure of the

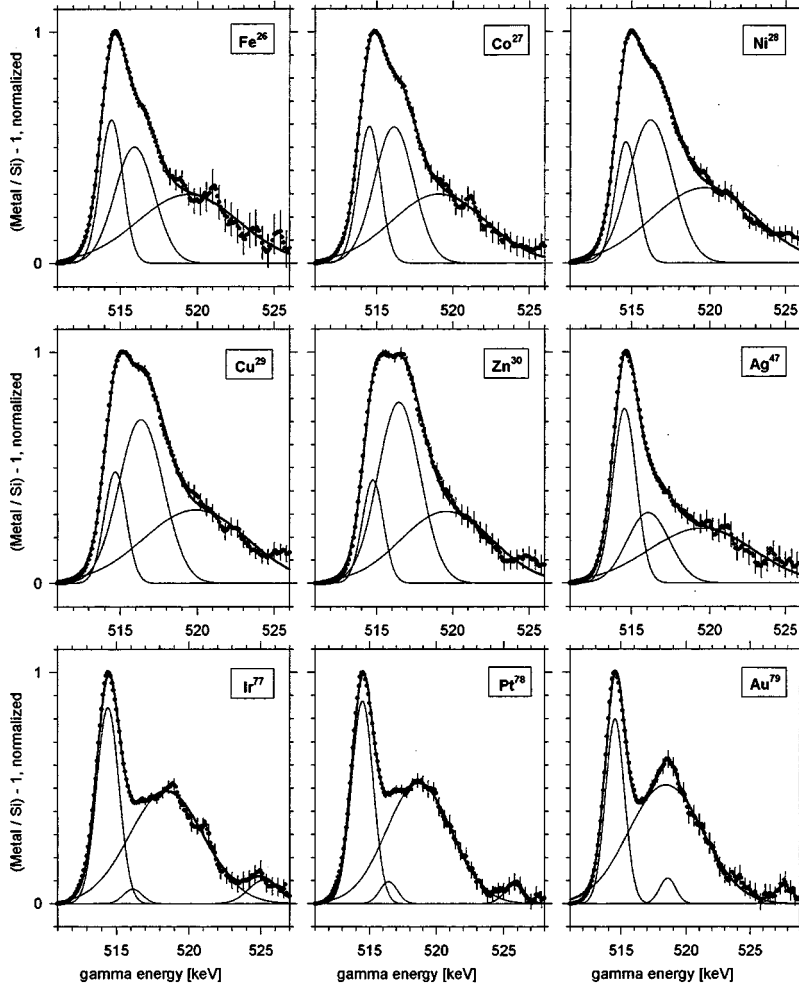


FIG. 5. Quotient spectra for the transition metals Fe . . . Zn, Ag, and Ir . . . Au, all divided by the standard Si spectrum. Here, after normalization to 2 in the maximum, the constant reference value 1 has been subtracted. The spectra were then fitted with 3 (Ir . . . Pt: 4) Gaussians (thin lines). Their sums, shown as the bold continuous lines, are practically indistinguishable from the corresponding measured spectra.

precision and repeatability of experiments by comparison with other published data, because it is difficult to meaningfully evaluate discrepancies between theory and experiment without a measure of the precision of the experimental work. We note that although our spectra for Ni and Cu are similar to those reported in Ref. 5, they are not identical. Variations between spectra obtained in different laboratories may be due to either differences in sample quality or in experimental conditions.

It is apparent from Refs. 4, 5, and 7 that agreement between theory and experiment is fair but not exact. Alatalo *et al.*<sup>4</sup> calculate annihilation peak shapes for Si, GaAs, and InP, but their calculations reproduce their measured peak shapes only in a qualitative way. Szpala *et al.*<sup>5</sup> do not attempt to match their spectra with theoretical predictions, but interpret their data based on experimental results only.

Asoka-Kumar *et al.*<sup>7</sup> show both experimentally obtained and theoretically calculated quotient spectra, but find only qualitative agreement. Here the situation might be more complicated, since annihilation peaks for two different materials have to be calculated quite accurately before a quotient spectrum can be reproduced reasonably well. If we compare our spectra for Fe, Ni, and Cu with their calculated ones [i.e., their Fig. 4(b)] and keep in mind that we divide by Si, while Asoka-Kumar *et al.* divide by Al (however, the spectra for Si and Al are fairly similar, as can be seen, e.g., from the Si/Al spectrum shown in Ref. 7), we find that their

calculations fit our experimental data somewhat better than their own measured spectra. This is true for both the general peak shapes (consisting obviously of two closely spaced contributions, the one centered at higher electron momenta growing in relative intensity with increasing  $Z$ ), and the maximum intensities of the quotient curves.

Although we introduced the 3 Gaussian fit only because of its apparent success in reproducing the measured spectra, the fits show features that seem at least qualitatively to change in a reasonable fashion. The fact that the center energies of the gaussian contributions increase with  $Z$  in the series of the  $3d$  metals is consistent with the shift of the atomic levels to higher binding energies for increasing  $Z$ . In Fig. 6(a) on the right side we show the kinetic energy of a free electron, which, upon annihilating with a resting positron, would create a  $\gamma$  ray with a maximum Doppler shifted energy as given on the left axis. The open symbols in that figure represent the  $M_I (=3s)$  and  $M_{II,III} (=3p)$  atomic energy levels,<sup>14</sup> using the virial theorem approximation that in the atom the kinetic energy of an electron  $E_{\text{kin}}$  equals the binding energy, and the electron momentum  $p_{\text{el}}$  can be calculated as  $p_{\text{el}} = \sqrt{2mE_{\text{kin}}}$ . While the energies of the  $3s$  electrons reasonably reproduce the experimental peak positions, the  $3p$  electrons do not fit the  $G_1$  peaks. Finally, there seems to be no level in the vicinity of the  $G_3$  peak, which may be an artefact of the quotient calculation.

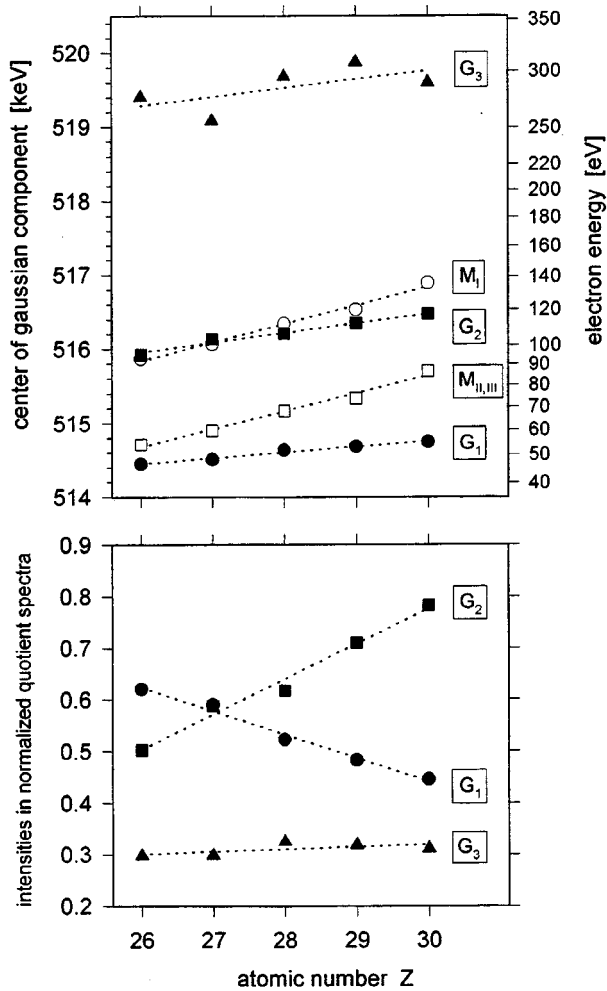


FIG. 6. Parameters of the 3 gaussians  $G_1 \dots G_3$  used for fitting the spectra of Fe, Co, Ni, Cu, and Zn in Fig. 5. (a) Center energies as a function of the atomic number  $Z$ . On the right-hand scale, the kinetic energy of a free electron that would cause such a  $\gamma$  energy when annihilating with a positron at rest, is displayed. Also, the atomic energy levels  $M_{II,III}$  and  $M_I$  (Ref. 14) are shown with open symbols. (b) Intensities of the three Gaussian components as a function of  $Z$ . In both graphs, the data are fit by straight lines (dotted).

The agreement is not exact, however we believe it is sufficient to allow the identification of spectral features with particular atomic subshells. We do not expect agreement at any level beyond this because (i) the virial theorem provides an estimate of the expectation value of the electron's kinetic energy, while the positron samples preferentially the lower-energy portion of the electron wave function (i.e., farther from the nucleus), (ii) dividing by the spectrum of silicon to obtain quotients may not exactly conserve the peak positions, and (iii) no effects such as positron-electron correlation are accounted for. We note that despite its simplicity, this model qualitatively explains aspects of the spectra and provides a direct physical interpretation.

Considering the relative intensities of the three gaussian contributions, Fig. 6(b) reveals that these can be fit convincingly with straight lines. The relative contribution of the  $G_1$  peak decreases with increasing  $Z$ , while  $G_2$  increases. An explanation of this behavior would have to take into consid-

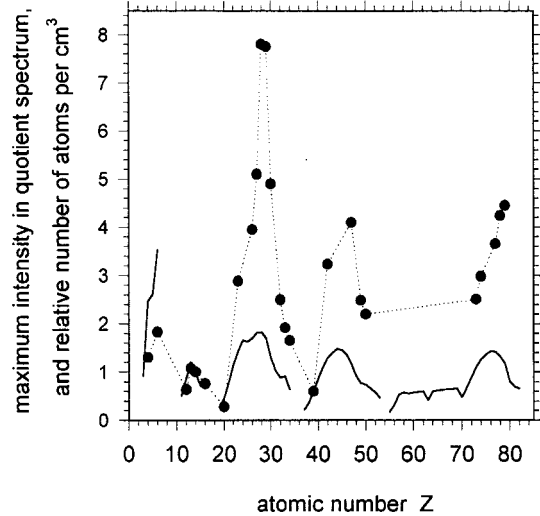


FIG. 7. Comparison of the intensity maxima in the measured quotient spectra (all divided by the Si standard) for 26 different pure elements (points), with the calculated relative atomic density (i.e., normalized to Si, solid line).

eration the relative density of  $3s$  and  $3p$  electrons at relatively large distances from the nucleus.  $G_3$ , on the other hand, maintains a constant intensity for all five elements.

The similarity of the Ag spectrum to the Fe . . . Zn spectra obviously is caused by the similarity in electronic structure. In the latter elements, the outer orbitals, i.e., valence electrons, are  $3d$  and  $4s$ , with  $3s$  and  $3p$  as the shallowest core levels. In Ag, the relevant core levels are  $4s$  and  $4p$ , while  $4d$  and  $5s$  constitute the valence electrons. Therefore, the Ag spectrum, too, can be fit in a similar manner with 3 gaussians, increasing in width with center energy. In contrast, the case of Ir, Pt, and Au is different, in that although  $5d$  and  $6s$  are the valence orbitals, the shallowest core levels are now  $4f$ . It is therefore not surprising that these spectra differ from those of the previous elements in their general shape, but on the other hand are similar to each other.

When it comes to interpreting the absolute intensities of the quotient spectra as depicted in Fig. 7, we have to keep in mind that these depend not only on the atomic properties, but also on the sample structure, especially the amount and size of vacancy-type defects present, since these reduce the core annihilation rate in favor of valence annihilations. Comparison with the theoretical predictions of Asoka-Kumar *et al.*, i.e., Fig. 4(b) in Ref. 7, is as follows: From this figure we extract for Cu, Ni, Fe, Ge, and Sn peak quotient values of 7.8, 6.2, 4.6, 2.1, and 2.0. Our measured values are 7.75, 7.8, 3.9, 2.5, and 2.2, respectively, indicating reasonable agreement.

In this work we have not addressed variations due to anisotropy of the electron momentum distribution. Angular correlation measurements<sup>15</sup> indicate that these effects are of the order of a few percent and are mainly confined to the low electron momentum region. Orientation effects are also reduced by the fact that the (cylindrical) detectors subtend a half angle of  $9^\circ$  and therefore average over a range of orientations.

Concluding, we find that even closely related elements

can be positively identified by their quotient spectra, if these are measured with sufficient precision. On the other hand, spectra of elements adjacent in the periodic table exhibit certain similarities and differ in a systematic way from each other. This information can be taken as an additional experimental input when attempting to theoretically predict annihilation  $\gamma$ -ray quotient spectra.

#### ACKNOWLEDGMENTS

We thank K. Griffiths (Department of Chemistry, UWO) for supplying most of the samples, and S. P. Goldman and R. A. Holt (Department of Physics and Astronomy, UWO) as well as K. G. Lynn (Washington State University) for helpful discussions.

---

\*Author to whom correspondence should be addressed: Uwe Myler. Tel. and FAX (same number): (519) 661-3463; Electronic address: umyler@julian.uwo.ca

- <sup>1</sup>P. J. Schultz and K. G. Lynn, *Rev. Mod. Phys.* **60**, 701 (1988).
- <sup>2</sup>R. N. West, *Adv. Phys.* **22**, 263 (1973).
- <sup>3</sup>D. W. Lawther and P. J. Simpson, *Defect Diffus. Forum* **138/139**, 1 (1996).
- <sup>4</sup>M. Alatalo, H. Kauppinen, K. Saarinen, M. J. Puska, J. Mäkinen, P. Hautojärvi, and R. M. Nieminen, *Phys. Rev. B* **51**, 4176 (1995).
- <sup>5</sup>S. Szpala, P. Asoka-Kumar, B. Nielsen, J. P. Peng, S. Hayakawa, K. G. Lynn, and H.-J. Gossmann, *Phys. Rev. B* **54**, 4722 (1996).
- <sup>6</sup>U. Myler, R. D. Goldberg, A. P. Knights, D. W. Lawther, and P. J. Simpson, *Appl. Phys. Lett.* **69**, 3333 (1996).
- <sup>7</sup>P. Asoka-Kumar, M. Alatalo, V. J. Ghosh, A. C. Kruseman, B. Nielsen, and K. G. Lynn, *Phys. Rev. Lett.* **77**, 2097 (1996).
- <sup>8</sup>U. Myler, P. J. Simpson, D. W. Lawther, and P. M. Rousseau, *J.*

*Vac. Sci. Technol. B* **15**, 757 (1997).

- <sup>9</sup>K. G. Lynn and A. N. Goland, *Solid State Commun.* **18**, 1549 (1976).
- <sup>10</sup>K. G. Lynn, J. R. MacDonald, R. A. Boie, L. C. Feldman, J. D. Gabbe, M. F. Robbins, E. Bonderup, and J. Golovchenko, *Phys. Rev. Lett.* **38**, 241 (1977).
- <sup>11</sup>J. R. MacDonald, K. G. Lynn, R. A. Boie, and M. F. Robbins, *Nucl. Instrum. Methods* **153**, 189 (1978).
- <sup>12</sup>K. G. Lynn, J. E. Dickman, W. L. Brown, M. F. Robbins, and E. Bonderup, *Phys. Rev. B* **20**, 3566 (1979).
- <sup>13</sup>P. J. Schultz, *Nucl. Instrum. Methods Phys. Res. B* **30**, 94 (1988).
- <sup>14</sup>*CRC Handbook of Chemistry and Physics*, 56th ed., edited by R. C. Weast (CRC, Cleveland, OH, 1975).
- <sup>15</sup>See, e.g., A. T. Stewart, J. B. Shand, J. J. Donaghy, and J. H. Kusmiss, *Phys. Rev.* **128**, 118 (1962); W. Triftshäuser and A. T. Stewart, *J. Phys. Chem. Solids* **32**, 2711 (1971).